

Article

# Developing Land-Use Regression Models to Estimate PM<sub>2.5</sub>-Bound Compound Concentrations

Chin-Yu Hsu <sup>1</sup>, Chih-Da Wu <sup>2,3,\*</sup>, Ya-Ping Hsiao <sup>1,2</sup>, Yu-Cheng Chen <sup>1,4</sup>, Mu-Jean Chen <sup>1</sup> and Shih-Chun Candice Lung <sup>5,6,7,\*</sup>

<sup>1</sup> National Institute of Environmental Health Sciences National Health Research Institutes, Miaoli 350, Taiwan; gracecyhsu@nhri.org.tw (C.-Y.H.); hsiaoyapiou@gmail.com (Y.-P.H.); yucheng@nhri.org.tw (Y.-C.C.); zeromagi@nhri.org.tw (M.-J.C.)

<sup>2</sup> Department of Forestry and Natural Resources, National Chiayi University, Chiayi 600, Taiwan

<sup>3</sup> Department of Geomatics, National Cheng Kung University, Tainan 701, Taiwan

<sup>4</sup> Department of Occupational Safety and Health, China Medical University, Taichung 404, Taiwan

<sup>5</sup> Research Center for Environmental Changes, Academia Sinica, Taipei 115, Taiwan

<sup>6</sup> Department of Atmospheric Sciences, National Taiwan University, Taipei 106, Taiwan

<sup>7</sup> Institute of Environmental Health, School of Public Health, National Taiwan University, Taipei 100, Taiwan

\* Correspondence: chidawu@mail.ncku.edu.tw (C.-D.W.); sclung@rcec.sinica.edu.tw (S.-C.C.L.);

Tel.: +886-6-275-7575 (ext. 63841) (C.-D.W.); +886-2-2653-9885 (ext. 277) (S.-C.C.L.);

Fax: +886-6-2375764 (C.-D.W.); +886-2-2783-3584 (S.-C.C.L.)

Received: 26 October 2018; Accepted: 4 December 2018; Published: 6 December 2018



**Abstract:** Epidemiology estimates how exposure to pollutants may impact human health. It often needs detailed determination of ambient concentrations to avoid exposure misclassification. However, it is unrealistic to collect pollutant data from each and every subject. Land-use regression (LUR) models have thus been used frequently to estimate individual levels of exposures to ambient air pollution. This paper used remote sensing and geographical information system (GIS) tools to develop ten regression models for PM<sub>2.5</sub>-bound compound concentration based on measurements of a six-year period including NH<sub>4</sub><sup>+</sup>, SO<sub>4</sub><sup>2-</sup>, NO<sub>3</sub><sup>-</sup>, OC, EC, Ba, Mn, Cu, Zn, and Sb. The explained variance (R<sup>2</sup>) of these LUR models ranging from 0.60 to 0.92 confirms that this study successfully estimated the fine spatial variability of PM<sub>2.5</sub>-bound compound concentrations in Taiwan where the distribution of traffic, industrial area, greenness, and culture-specific PM<sub>2.5</sub> sources like temples collected from GIS and remote sensing data were main variables. In particular, while they were much less used, this study showcased the necessity of remote sensing data of greenness in future LUR studies for reducing the exposure bias. In terms of local residents' health outcome or health effect indicators, this study further offers much-needed support for future air epidemiological studies. The results provide important insights into expanding the application of GIS and remote sensing on exposure assessment for PM<sub>2.5</sub>-bound compounds.

**Keywords:** fine particulate matter (PM<sub>2.5</sub>); land-use regression (LUR); compounds; culture-specific PM<sub>2.5</sub> sources; temples

## 1. Introduction

Fine particles dispersed in the atmosphere (PM<sub>2.5</sub>) are, in general, a mixture of different particle types with complex chemical compositions (such as ions, elementary and organic carbons, and metals). PM<sub>2.5</sub> can affect the atmospheric visibility, play key roles in the formation of acid rain and climate change, and deteriorate local and regional air quality. Exposure to ambient PM<sub>2.5</sub> is one leading factor in human health [1,2]. In addition, the potential impacts on human health may vary by the chemical compositions of particles, which not only affect toxicity by the presence of specific toxic elements,

but also influence the nonspecific toxicity of particles [3]. Particulate metals, which remain in the same form as they were emitted, might increase the possibility of lung or cardiopulmonary injuries and low birth weight [4,5]. Studies have suggested that chemical components of PM<sub>2.5</sub> are associated with mortality, including nitrates, sulfates, ammonium nitrate, elemental carbon (EC), organic carbon (OC), Fe, Ni, and Zn [6–8].

Recognizing the need for further research on PM characteristics and health, the Taiwan Environmental Protection Administration (EPA) has established two national monitoring networks for PM<sub>2.5</sub> that provide data on the chemical composition of PM in Northern and Southern Taiwan from 2002 to 2008. That said, it is still relatively unknown how long-term exposure to organic and inorganic compounds in PM may impact human health based on epidemiological studies [9]. Thus, more epidemiological studies on exposure to components of PM might be needed. When it comes to the study of the health impact of pollution exposure, the spatial variability of pollution concentration is essential.

Land-use regression (LUR) has been widely used to simulate pollution concentrations in the last decade because it can better represent small-scale spatial variability of long-term outdoor air pollution [10–12]. During the LUR model development processes, air pollutant levels measured from multiple locations are used as dependent variables and linked with a set of potentially land-use/land-cover related predictors to develop a multiple linear regression model for estimating air pollution at unmeasured sites [12–14].

Geographical information system (GIS) technologies provide flexible environments for collecting, storing, displaying, and analyzing distributions of emission sources necessary for LUR model development [15,16], such as road networks, which are usually considered the main factors in Western intra-urban PM<sub>2.5</sub> prediction, and culture-specific PM<sub>2.5</sub> sources like temples, which often affect Asian areas [12]. In addition, some studies have suggested that green spaces, including vegetation farms in urban areas, urban forests, and parks, can reduce particulate pollutants [12,17,18]. The efficiency with which to capture such particles varies with vegetation composition and by season [19,20]. However, previous LUR studies failed to consider the temporal variability of vegetation's capability to capture particles from the atmosphere and thus only used a single GIS thematic map to represent the allocation of parks or urban trees [21]. In recent years, remote sensing technologies have become readily available and can effectively provide large-scale and multitemporal surface information for many purposes, including forest greenness assessment [22]. However, they were rarely used to estimate nonmetal and metal compounds in PM<sub>2.5</sub> [23,24]. For example, only one case used vegetation information from remotely sensed images as a predictor in the development of a LUR model of PM<sub>2.5</sub> [12].

This paper adopts land-use regression models for the study of components of PM<sub>2.5</sub> based on measurements of a six-year period and remote sensing data in six sites across Taiwan. To further enhance the accuracy of such modeling, the distribution of temples collected from GIS maps, and greenness dynamics obtained from satellite image were applied as predictors in the modeling not only to represent the emission from Asian culture-specific sources, such as incense and joss money burning, but also to show the importance of the greenness variable to PM<sub>2.5</sub> compounds. The results provide important insights in expanding the application of GIS and remote sensing on exposure assessment for PM<sub>2.5</sub>-bound compounds.

## 2. Methods

### 2.1. Study Area and Material

Taiwan is an island country located in South East Asia, neighboring with China, Japan, and the Philippines. The population density in Taiwan has been estimated at 649 people per km<sup>2</sup> [25], ranking the 17th most heavily populated country in the world. Notably, there are 22 million registered motor vehicles (including both motorbikes and cars) in this small island, which means 91.5 vehicles per hundred people [26]. As a result, traffic emission is a significant factor of urban air pollution [27].

Moreover, in average, there are 2.31 factories per square kilometer and many of them are located near commercial districts and residential areas [28]. Local culture also plays a role in this study, as Taiwan has some unique emission sources of inorganic and organic components in PM<sub>2.5</sub>, such as the constant burning of joss paper and incense by thousands of temples and stir frying, a Chinese cooking technique used by almost all restaurants and households [29,30]. Additionally, one quarter of the land in Taiwan is a cultivated area and the growing of crops is commonly stimulated by fertilizers, such as potassium nitrate and ammonium sulfate [31]. These four main emission sources mentioned above not only elevate the level of pollutants, but also increase the difficulty in estimating the spatial–temporal variability of metal and nonmetal components in PM<sub>2.5</sub> in Taiwan.

## 2.2. Experimental Methods

To investigate the physical and chemical properties of aerosols in Taiwan, a sampling network consisting of six stations was initiated from 2002 to 2007. Figure 1 illustrates the geographical location of these stations. Fugueijiao is located at the northeast corner of Taiwan, along with urban/suburban stations in Taipei, Taichung, Tainan, and Pingtung, which lie in the western plains. These locations were chosen because they are highly developed, industrialized, and populated. On the other hand, the eastern measurement station is 10 km north from the downtown of Hualien, which is a rural area with less population and industry density.

The sampling period was usually 12 h: Daytime samples were collected from 8 a.m. to 8 p.m., and night-time sampling was from 8 p.m. to 8 a.m. the next day. Sometimes the sampling was conducted on a daily basis, i.e., from 8 a.m. to 8 a.m. the next day. Thus, in the following data analysis, we paired all the half-day measurements and integrated them to the daily measurements. We also excluded those unpaired data (i.e., without the day/night counterpart) in this study. Moreover, we did not include data for raining days, because precipitation can significantly suppress the formation of secondary organic carbon (SOC) [32,33].

Mass concentration of PM<sub>2.5</sub> was determined by gravimetric measurement of the samples collected on Polytetrafluoroethylene (PTFE) filters. The PTFE filter samples were then used for the analysis of soluble ions (Na<sup>+</sup>, NH<sub>4</sub><sup>+</sup>, SO<sub>4</sub><sup>2-</sup>, Cl<sup>-</sup>, NO<sub>3</sub><sup>-</sup>) using ion chromatograph and metals (Al, Ba, Ca, Cd, Cu, Fe, K, Mo, Mn, Na, Ni, Pb, Sb, Sr, Ti, and Zn) using inductively coupled plasma mass spectrometry. The samples for carbonaceous analysis were collected on quartz filters. Before sampling, all the filters were baked at 900 °C for 3 h to remove organic contaminants. The mass loadings of organic carbon (OC) and elemental carbon (EC) on the filter samples were analyzed using a DRI-2001A carbonaceous aerosol analyzer, following the IMPROVE thermo–optical reflectance (TOR) protocol [34]. More details are available in our previous studies [32,33].

Since we measured multiple compounds of PM<sub>2.5</sub> at each site, it is very complicated to analyze the spatial variation of each compound between any two sites. Thus, we simply compared the variation of the entire group of compounds between sites using the coefficient of divergence (CD; a self-normalizing parameter):

$$CD_{jk} = \sqrt{\frac{1}{p} \sum_{i=1}^p \left( \frac{x_{ij} - x_{ik}}{x_{ij} + x_{ik}} \right)^2}, \quad (1)$$

where *j* and *k* stand for two sampling sites, *p* is the number of investigated components, and *x*<sub>*ij*</sub> and *x*<sub>*ik*</sub> represent the average mass concentrations of a chemical component *i* at sites *j* and *k* [35]. If the CD approaches zero, the two sampling sites are similar (<0.3 was used in this study). If the CD approaches one, the two sampling sites are very different (> or = 0.3 was used in this study) [35].

The PM<sub>10</sub> was obtained from the EPA database. An unhealthy amount of PM<sub>10</sub> concentration was announced by the Taiwan EPA whenever local daily averaged concentrations exceeded 125 µg/m<sup>3</sup> (PM<sub>10</sub> episodes). The number of days for PM<sub>10</sub> episodes was also calculated as a predictor to see if this predictor would impact the concentration of PM<sub>2.5</sub>-bound compounds. The data of temperature,

rainfall, UV, and humidity were obtained from the Central Weather Bureau, Taiwan. Since the concentrations between  $PM_{10}$  and  $PM_{2.5}$  are highly correlated, we may use  $PM_{10}$  as a predictor variable to develop LUR models for estimating  $PM_{2.5}$ -bound compound concentrations.

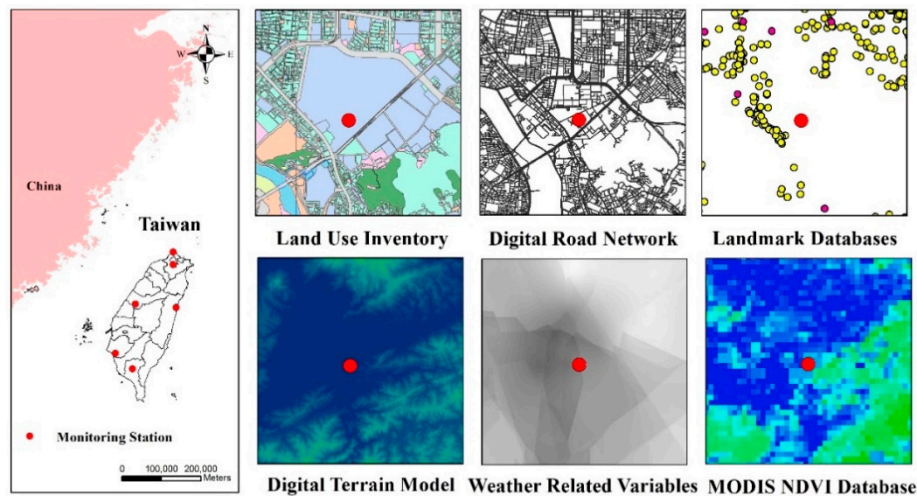


**Figure 1.** Overview of the six measurement sites and the illustrations of the collected geospatial databases.

### 2.3. Geospatial Database

To develop LUR models, we needed land-use or land-cover related information from several GIS layers and spatial databases. For instance, the Institute of Transportation of the Ministry of Transportation and Communication produced a GIS map with digital map data recording the spatial distribution of road networks with a polyline geofomat. All of the roads in the database were reclassified into two categories: Expressways versus others (e.g., local roads and main streets). To estimate the effects of traffic condition upon air quality, we calculated the density of all types of roads as well as each of two categories surrounding the measurement sites. We also used a 2010 database from the Industrial Development Bureau to determine the distance from each measurement site to the nearest industrial park. The second national land-use survey of 2007 recorded the land-use/land-cover information for Taiwan island-wide. For LUR modeling, we then selected several subtypes of land cover, such as residential areas, farms, water bodies, parks and greenbelts, railways, national airports, and sandstone fields from this database. Spatial distributions of temples and Chinese restaurants from the point of interest (POI) landmark database, and crematoriums from the Taiwan EPA environmental database were used for taking the culture-specific emissions into account. Moreover, the location of sewage treatment plants was also extracted from the Taiwan EPA environmental database for our analysis. A digital terrain model (DTM) with  $20\text{ m} \times 20\text{ m}$  resolution was applied to obtain the elevation above sea level of the measurement site. As coal-fired power plants contribute considerable air pollution, we collected the location of all coal-fired power plants in Taiwan from Google Maps to calculate the distance from each  $PM_{2.5}$  measurement site to the nearest coal-fired power plant. In addition to the GIS databases mentioned above, NASA's MODIS normalized difference vegetation index (NDVI) was also incorporated to represent the surrounding greenness during the study period. The spatial resolution of MODIS NDVI is  $250\text{ m} \times 250\text{ m}$ . NDVI images from 2000 to 2006 were all collected and aggregated to annual average for our analysis. We applied the Kriging interpolation model to simulate  $PM_{10}$  concentration and meteorological data nationwide from 76 Taiwan EPA air quality monitoring stations and 130 weather stations, respectively.

All of these geospatial predictor variables were abstracted from 25 m to 5000 m circular buffer ranges surrounding each  $PM_{2.5}$  measurement site to represent the land-use/land-cover allocations in the neighborhoods. Figure 1 thus shows the illustrations of the six measurements sites and the collected geospatial databases; Table 1 lists the potential predictor variables used in this study.

**Table 1.** List of potential predictor variables.

Variable Category	Variable	Data Description	Expected Direction	Data Type	Unit	Buffer
Taiwan EPA database	PM <sub>10</sub> (season)	cold and warm seasonally average	(+)	raster data	µg/m <sup>3</sup>	-
	PM <sub>10</sub> (year)	annual average	(+)	raster data	µg/m <sup>3</sup>	-
	PM <sub>10</sub> episode <sup>a</sup> (season)	number of days for PM <sub>10</sub> > 125 µg/m <sup>3</sup>	(+)	numerical data	day/season	-
	PM <sub>10</sub> episode <sup>a</sup> (year)	number of days for PM <sub>10</sub> > 125 µg/m <sup>3</sup>	(+)	numerical data	day/year	-
Central Weather Bureau database	Temperature (season)	cold and warm seasonally average	(+/-)	raster data	°C/season	-
	Temperature (year)	annual average	(+/-)	raster data	°C/year	-
	Rain fall (season)	cold and warm seasonally average	(-)	raster data	mm/season	-
	Rain fall (year)	annual average	(-)	raster data	mm/year	-
	UV (season)	cold and warm seasonally average	(+)	raster data	nm/year	-
	UV (year)	annual average	(+)	raster data	nm/year	-
	Humidity	annual average	(-)	raster data	%/year	-
Institute of Transportation digital map data (2006)	Local road	rural road, city road, industrial road and unnamed road	(+)	area source	m <sup>b</sup>	25–5000 m
	Main road	National highway, provincial highway, county road, city highway	(+)	area source	m <sup>b</sup>	25–5000 m
	All types of road	Local road + Mayor road	(+)	area source	m <sup>b</sup>	25–5000 m
Industrial Development Bureau industrial database (2010)	Industrial park	distance to the nearest landmark	(-)	area source	m <sup>b</sup>	25–5000 m
The second national land-use survey (2007)	Purely residential area	-	(+)	Area source	m <sup>2b</sup>	25–5000 m
	Commercial area	-	(+)	Area source	m <sup>2b</sup>	25–5000 m
	Industrial area	-	(+)	Area source	m <sup>2b</sup>	25–5000 m
	Residential mixed with commercial area	Residential area + Industrial area	(+)	Area source	m <sup>2b</sup>	25–5000 m
	All types of residential area	Purely residential area + Residential mixed with commercial area	(+)	Area source	m <sup>2b</sup>	25–5000 m
	Rice farm	-	(+/-)	Area source	m <sup>2b</sup>	25–5000 m
	Fruit orchard	-	(+/-)	Area source	m <sup>2b</sup>	25–5000 m

Table 1. Cont.

Variable Category	Variable	Data Description	Expected Direction	Data Type	Unit	Buffer
The second national land-use survey (2007)	Mixed farm	Rice farm + Fruit orchard	(+/-)	Area source	m <sup>2b</sup>	25–5000 m
	Water body	-	(-)	Area source	m <sup>2b</sup>	25–5000 m
	Park and greenbelt	-	(+)	Area source	m <sup>2b</sup>	25–5000 m
	Railway	distance to the measurement sites	(+)	Area source	m	-
	National airport	distance to the measurement sites	(-)	Area source	m	-
	Sandstone field	distance to the measurement sites	(+)	Area source	m	-
Point of interest (POI) landmark database (2008)	Temple	-	(+)	Point source	count	25–5000 m
	Chinese restaurant	Chinese restaurant + Night market	(+)	Point source	count	25–5000 m
Taiwan EPA environmental database	Crematorium	distance to the measurement sites	(-)	Point source	m	-
	Crematorium	distance to the measurement sites	(-)	Area source	m	-
	Industrial sewage treatment plant	distance to the measurement sites	(-)	Area source	m	-
	Domestic sewage treatment plant	distance to the measurement sites	(-)	Area source	m	-
Digital terrain model with 20 m resolution	Altitude	elevation above sea level of the measurement site	(+)	raster data	m	-
Vegetation indices from remote sensing	NDVI	-	(-)	raster data	unitless	-
Location of coal-fired power plants	Coal-fired power plants	distance to the measurement sites	(-)	Point source	m	-

<sup>a</sup> number of days for PM<sub>10</sub> episode; <sup>b</sup> buffers were set for 25, 50, 75, 100, 125, 150, 175, 200, 250, 500, 750, 1000, 1250, 1500, 1750, 2000, 3000, and 5000 m.

#### 2.4. LUR model Development and Validation

Land-use regression models were built following a methodology developed in our paper published earlier [12]. We used a supervised stepwise procedure to maximize the percentage of explained variability ( $R^2$ ). For all potential predictor variables, we chose an a priori direction of effect to each compound of  $PM_{2.5}$  concentration (e.g., positive for road length and industrial area, and both positive and negative directions for rice farms, fruit orchards, and forests) [24,36]. The model starts with the variable having not only the highest explained variance in a univariate analysis, but also a regression slope with the expected direction. Then, all other variables were added to this model separately by assessing if the  $p$ -value was  $<0.1$  and variance inflation factor (VIF) was  $<3$ . This procedure continues until none of the variables could fit the criteria mentioned above. Finally, we used  $R^2$ , adjusted  $R^2$ , and root mean square error (RMSE) to assess the model performance. A leave-one-out cross-validation (LOOCV) was further employed to confirm the model reliability and robustness. LOOCV essentially uses one observation as the validation data and the remaining observations as the training data for model development. The detailed methodology is available in our previous work [12].

### 3. Experimental Results

#### 3.1. Descriptive Statistics of $PM_{2.5}$ -Bound Compound Concentrations

The LUR model with  $R^2$  greater than 0.70 was considered to perform well, between 0.50 and 0.70 it was adequate, and less than 0.50 it was poor [24]. Because some compounds/elements ( $Na^+$ ,  $Cl^-$ , Al, Ca, Cd, Fe, K, Mo, Mn, Na, Ni, Pb, Sr, and Ti) performed poorly ( $R^2$  less than 0.5) for developing LUR in this study, we only show the  $PM_{2.5}$ -bound compound with  $R^2$  greater than 0.5 ( $NH_4^+$ ,  $SO_4^{2-}$ ,  $NO_3^-$ , OC, EC, Ba, Mn, Cu, Zn, and Sb) (see Figure 2). As expected, there were substantial differences by area (the results of CD range from 0.13 to 0.62 for the concentrations of  $PM_{2.5}$ -bound compositions), with rural areas (Fugueijiao and Hualien) having the lowest concentrations and the lowest within-area variability. As for the secondary aerosol ( $NH_4^+$ ,  $SO_4^{2-}$ ,  $NO_3^-$ , OC), the highest concentrations of  $NH_4^+$  and  $SO_4^{2-}$  were observed in Tainan, while the highest concentrations of  $NO_3^-$  and OC were observed in Pingtung. As for EC, the highest concentration was obtained in Taichung, followed by Taipei, Tainan, Pingtung, and two rural areas (Fugueijiao and Hualien). On the other hand, the OC/EC ratios fell within the range of 2.9–7.2. These values were consistent with those observed in a previous study conducted in Taichung, Changhua, and Yunlin in central Taiwan [33,37], which suggested a relatively high concentration of SOC in the study areas. Chou et al. (2010) [33] also indicated that the elevated concentrations of SOC were likely due to the increases in biogenic secondary organic aerosols precursors [38]. In addition, the secondary aerosol is likely caused by the following sources: Vehicle exhaust, coal combustion, biomass burning, oil burning, waste incineration, and household emission via their precursor gas-to-particle conversion. Indeed, the formation of the secondary aerosol depends on the concentrations of  $SO_2$ ,  $NO_x$ ,  $NH_3$  and organic compound and weather condition, such as relative humidity, temperature, OH/radiation, and nighttime chemistry via  $NO_3$  [39], each of which exhibits seasonal and regional variations. As for  $PM_{2.5}$ -bound metals, the highest concentrations of Ba, Cu, and Zn were obtained in Tainan, while the highest concentrations of Mn and Sb were observed in Taichung. We adopted the enrichment factor (EF) analysis to roughly delineate the crustal and anthropogenic sources for  $PM_{2.5}$  metals. The detailed method is available in our previous works [37,40]. In each area, Cu, Zn, Sb, and Mn (except for Mn in Pingtung with an EF value of 3) with higher EF values ( $\geq 5$ ) were predominantly from anthropogenic emissions. As for Ba concentration, it arises from anthropogenic emissions (EF values  $\geq 5$ ) at half the stations, while for Taichung and two rural areas (Fugueijiao and Hualien), the EF levels of 1.0–5.0 were considered to be from both anthropogenic and crustal sources.

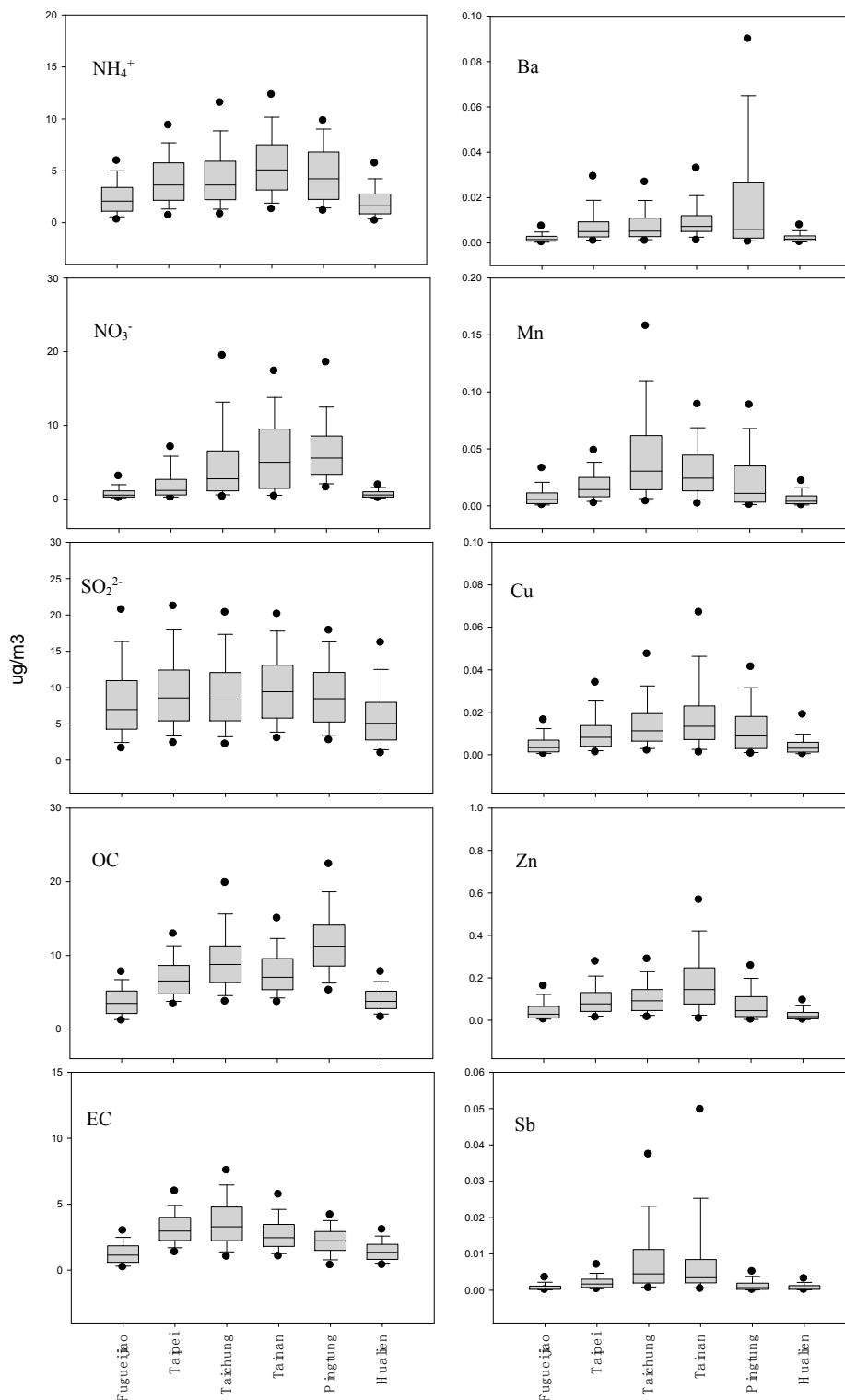


**Figure 2.** Box plots of the PM<sub>2.5</sub>-bound compounds in six study areas, including 5 and 95 percentiles (black dot), 25 and 75 percentiles respectively subtracted and added by inter-quartile range (lines outside the box), and 25 percentile, median and 75 percentile (box).

### 3.2. LUR Model Assessment

LUR models were developed for 10 PM<sub>2.5</sub> components. The coefficient estimate, partial R<sup>2</sup>, and overall performance are shown in Table 2 for nonmetal compounds and Table 3 for metal compounds. As predictors for LUR models, greenness and culturally specific sources, such as temples,

were contributors with either a positive or negative regression coefficient in the developed models. As for nonmetal compounds, the models performed well for  $\text{NH}_4^+$ ,  $\text{NO}_3^-$ , OC, and EC ( $R^2 > 0.70$ ), but performed lower than those for  $\text{SO}_4^{2-}$  ( $R^2 = 0.63$ ). In this study, the value of the model  $R^2$  for EC was 0.86, which demonstrated similar model performance to a previous study in ten European areas, where the model  $R^2$  was 0.87 [41]. On the other hand, the value of the model  $R^2$  for OC with 0.92 demonstrated better model performance than those in the European areas where the model  $R^2$  was 0.59 [41]. The difference of performance for compounds might be further affected by spatiotemporal variability [36,41]. In addition, Chou et al. (2010) [33] indicated that the biogenic secondary organic aerosols precursors would elevate SOC concentration [42]. Therefore, the model performance also depends on existing biogenic predictors. Regarding the LUR model for secondary inorganic aerosol ( $\text{NH}_4^+$ ,  $\text{NO}_3^-$ ,  $\text{SO}_4^{2-}$ ), however, we found no previous study on this topic.

As for metal compounds, the models performed well for Mn, Sb, and Zn ( $R^2 > 0.70$ ), but performed lower than those for Ba and Cu (see Table 2). Regarding Ba and Cu, the model  $R^2$  was 0.64 and 0.60, respectively, which were lower than the previous studies for Ba with 0.80 [24] and Cu between 0.70 and 0.80 [24,36]. However, these two studies [24,36] conducted sampling only in four weeks (January and August) or one year, while they disregarded other years and months with temporal variation of concentration. As a result, they cannot be used for estimating long-term concentration, which is fundamental for exposure assessment [11,12,43]. Regarding Mn and Sb, the model  $R^2$  was 0.76 and 0.82, which were similar to previous studies for Mn ( $R^2$  between 0.70 to 0.80) [24,44] and Sb ( $R^2$  equal to 0.75) [24]. As for Zn, the model  $R^2$  was 0.78, which was similar to previous studies in Canada and Australia with  $R^2$  values of 0.80 and 0.75, respectively [24,44], but greater than those in Taipei, Taiwan, and Europe with  $R^2$  equal to 0.57 and 0.67, respectively [37,45].

**Table 2.** Results of land-use regression (LUR) models for regression coefficient (partial  $R^2$ ) for non-metal  $\text{PM}_{2.5}$ -bound compound.

Variable	Log_EC	Log_OC	Log_SO <sub>4</sub> <sup>2-</sup>	Log_NH <sub>4</sub> <sup>+</sup>	Log_NO <sub>3</sub> <sup>-</sup>
Intercept	0.93	0.22	0.85	0.37	0.74
Local road_175		$3.92 \times 10^{-4}$ (0.81)			
All type of road_25					0.011 (0.09)
Residential mixed with Commercial area_500	$9.55 \times 10^{-7}$ (0.09)				
Temple_5000				0.002 (0.03)	
Domestic sewage treatment plant <sup>a</sup>				$-3.86 \times 10^{-6}$ (0.12)	
Rice farm mixed with fruit orchard_125		$1.04 \times 10^{-4}$ (0.02)			
Rice farm mixed with fruit orchard_175	$-2.25 \times 10^{-4}$ (0.73)		$-2.43 \times 10^{-7}$ (0.50)		
Rice farm mixed with fruit orchard_5000					$3.64 \times 10^{-7}$ (0.17)
Forest_1000					$-7.19 \times 10^{-8}$ (0.59)
NDVI_100			$-0.129$ (0.05)		
PM <sub>10</sub> (year)		0.004 (0.05)	0.003 (0.06)	0.02 (0.71)	
Rainfall (year)		$-0.02$ (0.02)			$-0.017$ (0.01)
Temperature (year)	$-0.02$ (0.04)		$-0.002$ (0.05)		
UV		0.08 (0.01)			
R <sup>2</sup> for model	0.86	0.92	0.63	0.87	0.90
Adj R <sup>2</sup> for model	0.85	0.90	0.60	0.86	0.89
LOOCV R <sup>2</sup>	0.78	0.84	0.53	0.82	0.83
RMSE	0.36	0.06	0.06	0.15	0.16

<sup>a</sup> distance to the nearest landmark.

**Table 3.** Results of LUR models for regression coefficient (partial R<sup>2</sup>) for metal PM<sub>2.5</sub>-bound compound.

Variable	Log_Ba	Log_Cu	Log_Mn	Log_Sb	Log_Zn
Intercept	−3.43	−0.04	−3.75	−2.99	1.82
Main road_4000	9.55 × 10 <sup>−6</sup> (0.13)				
All type of residential area_1750	2.53 × 10 <sup>−9</sup> (0.43)				
Industrial area mixed with commercial area_500	−1.27 × 10 <sup>−5</sup> (0.05)				
Industrial area mixed with commercial area_1250	2.18 × 10 <sup>−6</sup> (0.75)				
Industrial sewage treatment plant <sup>a</sup>	4.40 × 10 <sup>−6</sup> (0.15)				
Fossil fuel power plant <sup>a</sup>	0.19 (0.63)				
NDVI_1750	−0.61 (0.36)				
NDVI_125	−0.438 (0.03)				
PM <sub>10</sub> episode <sup>b</sup>	0.008 (0.03) 0.01 (0.12)				
PM <sub>10</sub> (annual average)	0.019 (0.51)				
Temperature	0.001 (0.06)				
UV	0.009 (0.11) 0.89 (0.20) 0.04 (0.04)				
R <sup>2</sup> for model	0.64	0.60	0.76	0.82	0.78
Adj R <sup>2</sup> for model	0.61	0.55	0.71	0.79	0.75
LOOCV R <sup>2</sup>	0.55	0.50	0.64	0.73	0.66
RMSE	0.24	0.0041	0.21	0.22	0.03

<sup>a</sup> distance to the nearest landmark; <sup>b</sup> number of days for PM<sub>10</sub> episode.

### 3.3. Spatiotemporal Variations of PM<sub>2.5</sub>-Bound Compounds

Figure 3 illustrates the annual average concentration for the entire study period, as simulated by the developed model. Red to blue/green on the maps represents the levels of each PM<sub>2.5</sub> compound, from high to low. Regarding nonmetal compounds, western and southern areas clearly have higher concentrations throughout the study period except for NO<sub>3</sub><sup>−</sup>, since the eastern area is mainly occupied by agricultural fields. In addition, southern areas presenting higher concentrations (except for EC, which is a primary pollutant) suggested a strong latitude gradient in secondary aerosol concentration. On the other hand, the metal compounds and EC show different patterns from each other. For instance, Ba and Cu concentrations present a higher level in the south, while EC, Mn, Sb and Zn show high concentrations in the particular areas. The resulting pattern of metal and EC concentrations across the island is likely caused by local emission sources, such as vehicular and industrial emissions and human and commercial activities. For instance, EC and Ba have been identified in previous studies as markers for traffic, vehicular emissions, or brake and tire wear [37,46]. Zn was ascribed to power plant emissions because a high portion of Zn is in coal ranges and most of the Zn evaporates and condenses onto the fly ash particles when coal is combusted at high temperatures (typically around 1500 °C). Manganese (Mn) has been identified as the main component in aerosols in the iron ore and steel industry [47,48]. Many studies have suggested a link between industrial emissions and a high concentration of Sb [49,50]. See and Balasubramanian (2008) [51] suggested that EC and Cu could be released into the air through cooking exhaust hoods.

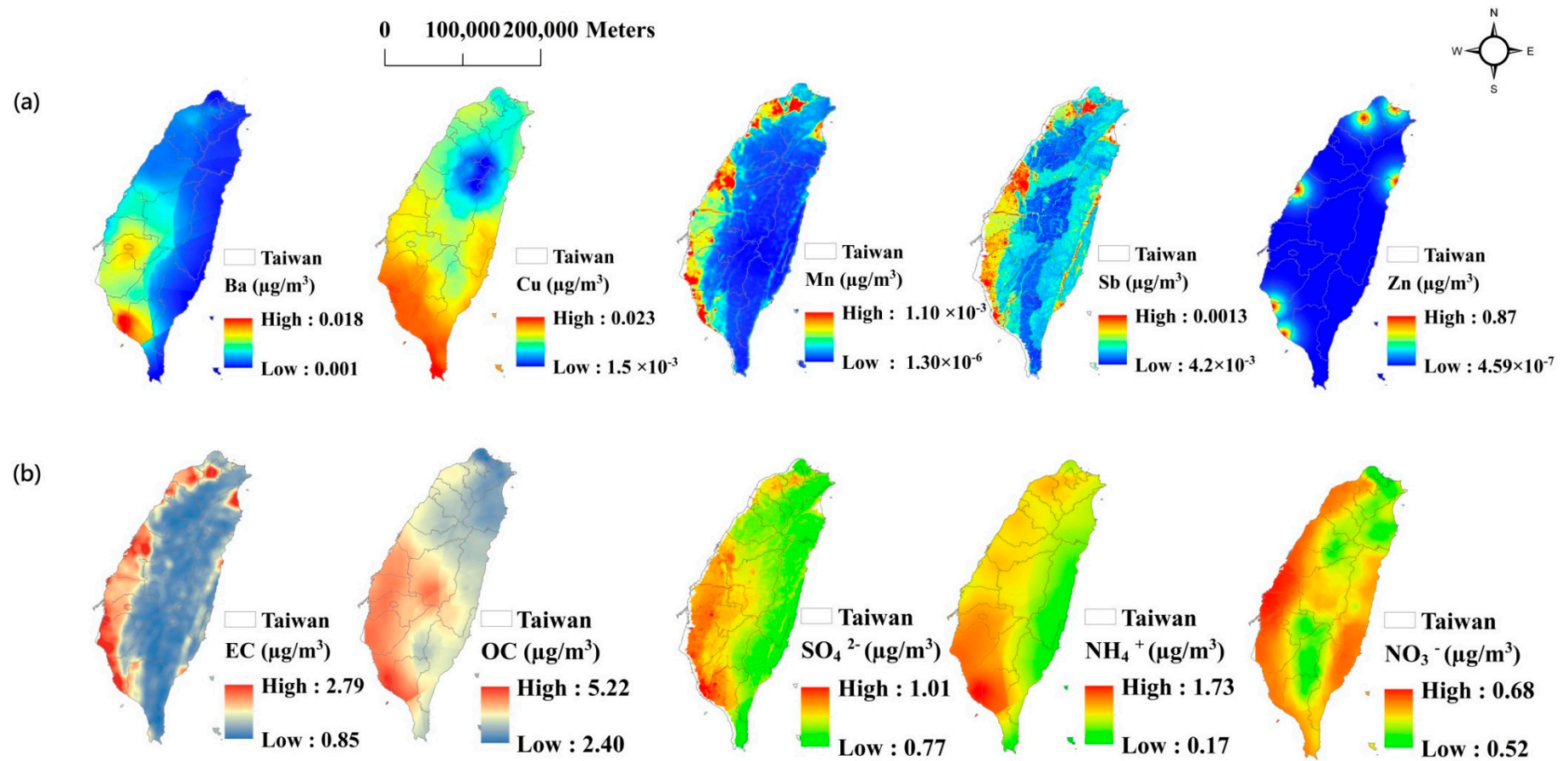


Figure 3. Annual average concentration of PM<sub>2.5</sub>-bound (a) nonmetal and (b) metal compounds simulated by the developed model.

#### 4. Discussion

While the LUR model has become increasingly popular to simulate air pollutant concentration, it is rarely used in Asia, including Taiwan [12,36]. This also means a limited understanding of PM<sub>2.5</sub> constituent characteristics in Asia and their association with local emission sources. This paper, thus, exploited LUR models coupled with GIS and remote sensing data for PM<sub>2.5</sub>-bound compound concentrations in Taiwan, which may represent typical Asian characteristics. This is also significant for the epidemiological studies in Asia, which need data with fine-scale exposure concentration.

Previous studies have shown that green space is associated with lower exposure to ambient air pollutants [20,52]. Actually, tree species and vegetation composition could efficiently capture pollutants [20,53]. For example, Yin et al. (2011) [53] demonstrated that the concentrations of PM, SO<sub>2</sub>, and NO<sub>2</sub> decreased 9.10%, 5.30%, and 2.60%, respectively, at distances of 50 to 100m from an urban woodland area. Nowak et al. (2006) [17] demonstrated that urban trees and shrubs could remove about 215,000 tons of PM<sub>10</sub> every year in the USA as a whole. Today, remote sensing technologies have become readily available to obtain greenness information from satellite images. In our study, long-term NDVI data coupled with buffer size analysis were used to assess plant growth (vigor) and neighborhood vegetation cover during the study years. The results of the negative regression coefficient for NDVI were obtained in the SO<sub>4</sub><sup>2-</sup>, Mn, and Sb LUR models. Moreover, the partial R<sup>2</sup> of NDVI in the Mn model was 0.36, indicating 36% of PM<sub>2.5</sub>-bound Mn variation could be explained by NDVI information in the developed LUR model. The aforementioned results demonstrate that NDVI information is an applicable factor in developing LUR models for compounds in fine particles.

On the other hand, there were large amounts of ammonia in East Asia atmosphere as a result of using fertilization in agricultural fields, which elevated NO<sub>3</sub><sup>-</sup> [54]. In addition, secondary organic carbons would increase due to the increases in biogenic secondary organic aerosols precursors, such as carbonaceous aerosols [33,38]. Carbonaceous aerosols are mainly emitted either directly through primary emissions or indirectly through gas-phase oxidation products from biogenic volatile organic compounds (BVOCs) [55,56]. BVOCs are primarily emitted from plants as a tool for communication and to handle biotic and abiotic stress [57,58]. On the other hand, the ability of green spaces, like vegetation planted in urban areas, urban forests, and parks, to remove particle pollutants has been well documented [17,18]. Thus, rice farms, fruit orchards, and forests had either a positive or negative regression coefficient to OC and NO<sub>3</sub><sup>-</sup> concentrations.

Population variables were included in the EC, NH<sub>4</sub><sup>+</sup>, and Cu models. This predictor variable represented various human and commercial activities, such as heating, cooking, and cleaning activities [51,59]. For instance, the aminium salts contained in the commercial degreaser solution are released into the air when people use a degreaser to clean kitchens [59]. Road length was also included in the OC, NO<sub>3</sub><sup>-</sup>, and Ba models. This predictor suggests traffic-related emission, such as vehicle exhaust and road dust re-suspended by automobiles and wind. Laboratory experiments have indicated that OC can be formed from photooxidation of precursors present in gasoline fuel and diesel exhaust. In addition, emissions from gasoline and diesel vehicles contain a certain amount of primary OC (POC) [42] and nitrogen oxides (NO<sub>x</sub>), which are the precursor of NO<sub>3</sub><sup>-</sup>. In addition, Amato et al. (2011) [60] suggested Ba comes from re-suspended dust.

While industry and traffic are often the dominant factors to estimate PM<sub>2.5</sub>-bound compounds [24,45], some culturally specific PM<sub>2.5</sub> sources must also be considered in Asia. Joss paper and incense burning are very important for many Asian households and temples for religious purposes [61], and several studies have shown their contributions to air pollution [27,62]. However, none of these studies considered joss paper and incense burning related variables to develop an LUR model for the concentration of PM<sub>2.5</sub>-bound compounds. In this study, we used the number of temples to reflect local emissions by joss paper and incense burning, which proved to be a significant predictor in our newly developed model (such as NH<sub>4</sub><sup>+</sup>). Thus, we would suggest future studies could consider this unique local cultural source as a predictor when establishing LUR models for estimating the concentration of PM<sub>2.5</sub>-bound compounds in other Asian regions.

The present study relied on the data collected at six sampling sites from 2002 to 2007. While a larger number of sampling sites is preferred, the comprehensive data measured and collected throughout a six-year period were still very helpful to serve our purpose. In addition, to sample and analyze PM-bound compound is often time-consuming and very expensive. Thus, it's not easy to have a six-year period of PM<sub>2.5</sub>-bound compound concentrations as used in this study. On the other hand, this study has some other limitations with regard to when we selected predictors. For instance, the comprehensive traffic count data and the number of buildings or the population, while often used by others to improve model performance [63,64], were not considered in this study because these data are not readily available in Taiwan. Nonetheless, compared to a one-year period (or shorter) of data used by others, this model chose a comprehensive data set covering the entire island throughout a six-year period to represent not only the spatial, but also temporal variation of compound concentrations in all locations of Taiwan. In addition, using such a long span of pollutant data in Taiwan to establish multiple LUR models with culturally specific and greenness predictors, these models showcased a mid-high estimation performance level, which can be used to better depict the concentration variation of PM<sub>2.5</sub>-bound constituent in Asian cities.

## 5. Conclusions

Land-use regression (LUR) models have thus been used frequently to estimate individual levels of exposures to ambient air pollution. The remote sensing data have become important for developing LUR models. This paper thus exploited LUR models with the remote sensing data for PM<sub>2.5</sub>-bound compound concentrations in Taiwan where traffic, industrial area, and greenness were the main variables. Using data from six measurement stations, we confirmed that the LUR models developed in this study can estimate fine spatial variability of long-term PM<sub>2.5</sub>-bound compound concentrations with the estimated uncertainty as low as 8% (e.g., for the estimation of OC compound). Moreover, this LUR method could be similarly used in future studies to develop new LUR models for other pollutants in Taiwan. In terms of local residents' health outcome or health effect indicators, this study further offers much-needed support for future air epidemiological studies.

**Author Contributions:** Conceptualization, Chih-Da Wu and Yu-Cheng Chen; Formal analysis, Chin-Yu Hsu and Ya-Ping Hsio; Funding acquisition, Chih-Da Wu and Shih-Chun Candice Lung; Investigation, Chin-Yu Hsu and Mu-Jean Chen; Methodology, Chih-Da Wu and Mu-Jean Chen; Project administration, Shih-Chun Candice Lung; Software, Ya-Ping Hsio; Writing—original draft, Chin-Yu Hsu and Chih-Da Wu; Writing—review & editing, Chih-Da Wu, Ya-Ping Hsio, Yu-Cheng Chen, Mu-Jean Chen and Shih-Chun Candice Lung.

**Funding:** This research was funded by the Ministry of Science and Technology [MOST 107-2119-M-006-030] and Academia Sinica [AS-107-SS-A03].

**Acknowledgments:** We appreciate the data support from the Research Center for Environmental Changes, Academia Sinica. We also thank the anonymous reviewers for their constructive comments on the early manuscript of this paper. Its contents are solely the responsibility of the authors and do not necessarily represent the official views of the funding agencies. The funding agencies had no role in the study design, data collection and analysis, decision to publish, or preparation of the manuscript.

**Conflicts of Interest:** The authors declare no conflict of interest.

## References

1. Dockery, D.W.; Pope, C.; Xu, X.; Spengler, J.; Ware, J.; Fay, M.; Ferris, B.; Speizer, F. An association between air pollution and mortality in six U.S. cities. *N. Engl. J. Med.* **1993**, *329*, 1753–1759. [[CrossRef](#)] [[PubMed](#)]
2. Cascio, W.E.; Katwa, L.C.; Linn, W.S.; Stram, D.O.; Zhu, Y.; Cascio, J.L.; Hinds, W.C. Effects of vehicle exhaust in aged adults riding on Los Angeles Freeways. *Am. J. Respir. Crit. Care Med.* **2009**, *179*, A1175.
3. Spurny, K.R. On the physics, chemistry and toxicology of ultrafine anthropogenic atmospheric aerosols (UAAA): New advances. *Toxicol. Lett.* **1998**, *96*, 253–261. [[CrossRef](#)]
4. Bell, M.L.; Belanger, K.; Ebisu, K.; Gent, J.F.; Lee, H.J.; Koutrakis, P.; Leaderer, B.P. Prenatal exposure to fine particulate matter and birth weight: variations by particulate constituents and sources. *Epidemiology* **2010**, *21*, 884–891. [[CrossRef](#)] [[PubMed](#)]

5. Gehring, U.; Beelen, R.; Eeftens, M.; Hoek, G.; de Hoogh, K.; de Jongste, J.C.; Keuken, M.; Koppelman, G.H.; Meliefste, K.; Oldenwening, M.; et al. Particulate Matter Composition and Respiratory Health: The PIAMA Birth Cohort Study. *Epidemiology* **2015**, *26*, 300–309. [[CrossRef](#)]
6. Fairley, D. Daily mortality and air pollution in Santa Clara County, California: 1989–1996. *Environ. Health Perspect.* **1999**, *107*, 637–641. [[CrossRef](#)]
7. Burnett, R.T.; Brook, J.; Dann, T.; Delocla, C.; Philips, O.; Cakmak, S.; Vincent, R.; Goldberg, M.S.; Krewski, D. Association between particulate- and gasphase components of urban air pollution and daily mortality in eight Canadian cities. *Inhal. Toxicol.* **2000**, *12*, S15–39. [[CrossRef](#)]
8. Ostro, B.; Feng, W.Y.; Broadwin, R.; Green, S.; Lipsett, M. The effects of components of fine particulate air pollution on mortality in California: Results from CALFINE. *Environ. Health Perspect.* **2007**, *115*, 13–19. [[CrossRef](#)]
9. USEPA. Air Explorer. Available online: <http://www.epa.gov/airexplorer> (accessed on 13 December 2006).
10. Guerschman, J.P.; Paruelo, J.M.; Bela, C.D.; Giallorenzi, M.C.; Pacin, F. Land cover classification in the Argentine Pampas using multi-temporal Landsat TM data. *Int. J. Remote Sens.* **2003**, *24*, 3381–3402. [[CrossRef](#)]
11. Pan, W.C.; Wu, C.D.; Chen, M.J.; Huang, Y.T.; Chen, C.J.; Su, H.J.; Yang, H.I. Fine particle pollution, alanine transaminase, and liver cancer: A Taiwanese prospective cohort study (REVEAL-HBV). *J. Natl. Cancer Inst.* **2016**, *108*. [[CrossRef](#)]
12. Wu, C.D.; Chen, Y.C.; Pan, W.C.; Zeng, Y.T.; Chen, M.J.; Guo, Y.L.; Lung, S.C. Land-use regression with long-term satellite-based greenness index and culture-specific sources to model PM<sub>2.5</sub> spatial—Temporal variability. *Environ. Pollut.* **2017**, *224*, 148–157. [[CrossRef](#)]
13. Wang, R.; Henderson, S.B.; Sbihi, H.; Allen, R.W.; Brauer, M. Temporal stability of land use regression models for traffic-related air pollution. *Atmos. Environ.* **2013**, *64*, 312–319. [[CrossRef](#)]
14. Aguilera, I.; Eeftens, M.; Meier, R.; Ducret-Stich, R.E.; Schindler, C.; Ineichen, A.; Phuleria, H.C.; Probst-Hensch, N.; Tsai, M.-Y.; Künzli, N. Land use regression models for crustal and traffic-related PM<sub>2.5</sub> constituents in four areas of the SAPALDIA study. *Environ. Res.* **2015**, *140*, 377–384. [[CrossRef](#)] [[PubMed](#)]
15. Demers, M.N. *Fundamentals of Geographic Information Systems*; John Wiley Sons, Inc.: New York, NY, USA, 2005.
16. Wu, Q.; Li, H.Q.; Wang, R.S.; Paulussen, J.; He, H.; Wang, M.; Wang, B.H.; Wang, Z. Monitoring and predicting land use change in Beijing using remote sensing and GIS. *Landsc. Urban Plan.* **2006**, *78*, 322–333. [[CrossRef](#)]
17. Nowak, D.J.; Crane, D.E.; Stevens, J.C. Air pollution removal by urban trees and shrubs in the United States. *Urban For. Urban Green.* **2006**, *4*, 115–123. [[CrossRef](#)]
18. McDonald, J.D.; Reed, M.D.; Campen, M.J.; Barrett, E.G.; Seagrave, J.; Mauderly, J.L. Health effects of inhaled gasoline Engine emissions. *Inhal. Toxicol.* **2007**, *19*, 107–116. [[CrossRef](#)] [[PubMed](#)]
19. Burkhardt, J. Hygroscopic particles on leaves: Nutrients or desiccants? *Ecol. Monogr.* **2010**, *80*, 369–399. [[CrossRef](#)]
20. Sæbø, A.; Popek, R.; Nawrot, B.; Hanslin, H.M.; Gawronska, H.; Gawronski, S.W. Plant species differences in particulate matter accumulation on leaf surfaces. *Sci. Total. Environ.* **2012**, *427*, 347–354. [[CrossRef](#)]
21. Kerckhoffs, J.; Wang, M.; Meliefste, K.; Malmqvist, E.; Fischer, P.A.H.; Janssen, N.; Beelen, R.; Hoek, G. A national fine spatial scale land-use regression model for ozone. *Environ. Res.* **2015**, *140*, 440–448. [[CrossRef](#)]
22. Wu, C.D.; McNeely, E.; Cedeño-Laurent, J.G.; Pan, W.C.; Adamkiewicz, G.; Dominici, F.; Candice Lung, S.C.; Su, H.-J.; Spengler, J.D. Linking Student Performance in Massachusetts Elementary Schools with the “Greenness” of School Surroundings Using Remote Sensing. *PLoS ONE* **2014**, *9*, e108548. [[CrossRef](#)]
23. Urman, R.; Gauderman, J.; Fruin, S.; Lurmann, F.; Liu, F.; Hosseini, R.; Franklin, M.; Avol, E.; Penfold, B.; Gilliland, F.; et al. Determinants of the spatial distributions of elemental carbon and particulate matter in eight Southern Californian communities. *Atmospheric environment. Atmos. Environ.* **2014**, *86*, 84–92. [[CrossRef](#)] [[PubMed](#)]
24. Zhang, J.J.Y.; Sun, L.; Barrett, O.; Bertazzon, S.; Underwood, F.E.; Johnson, M. Development of land-use regression models for metals associated with airborne particulate matter in a North American city. *Atmos. Environ.* **2015**, *106*, 165–177. [[CrossRef](#)]
25. DGB. Close DGB (Directorate General of Budget) National Statistics—Current Index. Available online: <http://www.stat.gov.tw/point.asp?index=4> (accessed on 9 August 2018).

26. MOTC (Ministry of Transportation and Communications). Vehicle Statistics. Available online: <http://www.motc.gov.tw/ch/home.jsp?id=6&parentpath=02017> (accessed on 9 August 2018).
27. Lung, S.C.C.; Hsiao, P.K.; Wen, T.Y.; Liu, C.H.; Fu, C.B.; Cheng, Y.T. Variability of intra-urban exposure to particulate matter and CO from Asian-type community pollution sources. *Atmos. Environ.* **2014**, *83*, 6–13. [[CrossRef](#)]
28. EPA (Environmental Protection Agency). PM<sub>2.5</sub> Automatic Monitoring. Available online: <http://taqm.epa.gov.tw/pm25/en/PM25A.aspx> (accessed on 9 October 2018).
29. Kuo, S.C.; Tsai, Y.I.; Sopajaree, K. Emission identification and health risk potential of allergy-causing fragrant substances in PM<sub>2.5</sub> from incense burning. *Build. Environ.* **2015**, *87*, 23–33. [[CrossRef](#)]
30. Yu, K.P.; Yang, K.R.; Chen, Y.C.; Gong, J.Y.; Chen, Y.P.; Shih, H.C.; Lung, S.-C.C. Indoor air pollution from gas cooking in five Taiwanese families. *Build. Environ.* **2015**, *93*, 258–266. [[CrossRef](#)]
31. Liou, R.M.; Huang, S.N.; Lin, C.W. Methane emission from fields with differences in nitrogen fertilizers and rice varieties in Taiwan paddy soils. *Chemosphere* **2003**, *50*, 237–246. [[CrossRef](#)]
32. Chou, C.C.-K.; Lee, C.-T.; Yuan, C.S.; Hsu, W.C.; Hsu, S.C.; Liu, S.C. Implications of the chemical transformation of Asian outflow aerosols for the long-range transport of inorganic nitrogen species. *Atmos. Environ.* **2008**, *42*, 7508–7519. [[CrossRef](#)]
33. Chou, C.C.K.; Lee, C.T.; Cheng, M.T.; Yuan, C.S.; Chen, S.J.; Wu, Y.L.; Hsu, W.C.; Lung, S.C.; Hsu, S.C.; Lin, C.Y.; et al. Seasonal variation and spatial distribution of carbonaceous aerosols in Taiwan. *Atmos. Chem. Phys.* **2010**, *10*, 9563–9578. [[CrossRef](#)]
34. Chow, J.; Watson, J.; Lowenthal, D.H.; Merrifield, T. Comparison of IMPROVE and NIOSH carbon measurements. *Aerosol Sci. Technol.* **2001**, *34*, 23–34. [[CrossRef](#)]
35. Zhang, Z.; Friedlander, S.K. A comparative study of chemical databases for fine particle Chinese aerosols. *Environ. Sci. Technol.* **2000**, *34*, 4687–4697. [[CrossRef](#)]
36. Ho, C.C.; Chan, C.C.; Cho, C.W.; Lin, H.I.; Lee, J.H.; Wu, C.F. Land use regression modeling with vertical distribution measurements for fine particulate matter and elements in an urban area. *Atmos. Chem.* **2015**, *104*, 256–263. [[CrossRef](#)]
37. Hsu, C.Y.; Chiang, H.C.; Chen, M.J.; Chuang, C.Y.; Tsen, C.M.; Fang, G.C.; Tsai, Y.I.; Chen, N.T.; Lin, T.Y.; Lin, S.L.; et al. Ambient PM<sub>2.5</sub> in the residential area near industrial complexes: Spatiotemporal variation, source apportionment, and health impact. *Sci. Total Environ.* **2017**, *590*, 204–214. [[CrossRef](#)] [[PubMed](#)]
38. Bencs, L.; Ravindra, K.; de Hoog, J.; Rasoazanany, E.O.; Deutsch, F.; Bleux, N.; Berghmans, P.; Roekens, E.; Krata, A.; Van Grieken, R. Mass and ionic composition of atmospheric fine particles over Belgium and their relation with gaseous air pollutant. *Environ. Monit.* **2008**, *10*, 1148–1157. [[CrossRef](#)]
39. Heo, J.B.; Hopke, P.K.; Yi, S.M. Source apportionment of PM<sub>2.5</sub> in Seoul, Korea. *Atmos. Chem. Phys.* **2009**, *9*, 4957–4971. [[CrossRef](#)]
40. Chen, Y.C.; Hsu, C.Y.; Lin, S.L.; Chang-Chien, G.P.; Chen, M.J.; Fang, G.C.; Chiang, H.C. Characteristics of Concentrations and Metal Compositions for PM<sub>2.5</sub> and PM<sub>2.5-10</sub> in Yunlin County, Taiwan during Air Quality Deterioration. *Aerosol Air Qual. Res.* **2015**, *15*, 2571–2583. [[CrossRef](#)]
41. Jedynska, A.; Hoek, G.; Wang, M.; Eeftens, M.; Cyrys, J.; Keuken, M.; Ampe, C.; Beelen, R.; Cesaroni, G.; Forastiere, F.; et al. Development of Land Use Regression Models for Elemental, Organic Carbon, PAH, and Hopanes/Steranes in 10 ESCAPE/TRANSPHORM European Study Areas. *Environ. Sci. Technol.* **2014**, *48*, 14435–14444. [[CrossRef](#)] [[PubMed](#)]
42. Ban-Weiss, G.A.; McLaughlin, J.P.; Harley, R.A.; Lunden, M.M.; Kirchstetter, T.W.; Kean, A.J.; Strawa, A.W.; Stevenson, E.D.; Kendall, G.R. Long-term changes in emissions of nitrogen oxides and particulate matter from on-road gasoline and diesel vehicles. *Atmos. Environ.* **2008**, *42*, 220–232. [[CrossRef](#)]
43. USEPA. User's Guide/Technical Backgrounddocument for US EPA Region 9's RSL (Regional Screening Levels) Tables. Available online: <http://www.epa.gov/region9/superfund/prg/> (accessed on 17 September 2018).
44. Dirgawati, M.; Heyworth, J.S.; Wheeler, A.J.; McCaul, K.A.; Blake, D.; Boeyen, J.; Cope, M.; Yeap, B.B.; Nieuwenhuijsen, M.; Brunekreef, B.; et al. Development of Land Use Regression models for particulate matter and associated components in a low air pollutant concentration airshed. *Atmos. Environ.* **2016**, *144*, 69–78. [[CrossRef](#)]
45. De Hoogh, K.; Wang, M.; Adam, M.; Badaloni, C.; Beelen, R.; Birk, M.; Cesaroni, G.; Cirach, M.; Declercq, C.; Dedele, A.; et al. Development of land use regression models for particle composition in twenty study areas in Europe. *Environ. Sci. Technol.* **2013**, *47*, 5778–5786. [[CrossRef](#)]

46. Varrica, D.; Bardelli, F.; Dongarra, G.; Tamburo, E. Speciation of Sb in airborne particulate matter, vehicle brake linings, and brake pad wear residues. *Atmos. Environ.* **2013**, *64*, 18–24. [[CrossRef](#)]
47. Querol, X.; Viana, M.; Alastuey, A.; Amato, F.; Moreno, T.; Castillo, S.; Pey, J.; de la Rosa, J.; Sánchez de la Campa, A.; Artíñano, B.; et al. Source origin of trace elements in PM from regional background, urban and industrial sites of Spain. *Atmos. Environ.* **2007**, *41*, 7219–7231. [[CrossRef](#)]
48. Cheng, K.; Wang, Y.; Tian, H.; Gao, X.; Zhang, Y.; Wu, X.; Zhu, C.; Gao, J. Atmospheric emission characteristics and control policies of five precedent-controlled toxic heavy metals from anthropogenic sources in China. *Environ. Sci. Technol.* **2015**, *49*, 1206–1214. [[CrossRef](#)] [[PubMed](#)]
49. Mokhtara, M.M.; Taiba, R.M.; Hassima, M.H. Understanding selected trace elements behavior in a coal-fired power plant in Malaysia for assessment of abatement technologies. *J. Air Waste Manag.* **2014**, *64*, 867–878. [[CrossRef](#)]
50. Das, R.; Khezri, B.; Srivastava, B.; Datta, S.; Sikdar, P.K.; Webster, R.D.; Wang, X.F. Trace element composition of PM<sub>2.5</sub> and PM<sub>10</sub> from Kolkata—A heavily polluted Indian metropolis. *Atmos. Pollut. Res.* **2015**, *6*, 742–750. [[CrossRef](#)]
51. See, S.W.; Balasubramanian, R. Chemical characteristics of fine particles emitted from different gas cooking methods. *Atmos. Environ.* **2008**, *42*, 8852–8862. [[CrossRef](#)]
52. Laforteza, R.; Carrus, G.; Sanesi, G.; Davies, C. Benefits and well-being perceived by people visiting green spaces in periods of heat stress. *Urban. For. Urban. Green.* **2009**, *8*, 97–108. [[CrossRef](#)]
53. Yin, S.; Shen, Z.; Zhou, P.; Zou, X.; Che, S.; Wang, W. Quantifying air pollution attenuation within urban parks: An experimental approach in Shanghai, China. *Environ. Pollut.* **2011**, *159*, 2155–2163. [[CrossRef](#)]
54. Kim, J.Y.; Song, C.H.; Ghim, Y.S.; Won, J.G.; Yoon, S.C.; Carmichael, G.R.; Woo, J.H. An investigation on NH<sub>3</sub> emissions and particulate NH<sub>4</sub><sup>+</sup> 4 -NO<sub>3</sub> formation in East Asia. *Atmos. Environ.* **2006**, *40*, 2139–2150. [[CrossRef](#)]
55. Genberg, J.; Hyder, M.; Stenstrom, K.; Bergstrom, R.; Simpson, D.; Fors, E.O.; Jonsson, J.A.; Swietlicki, E. Source apportionment of carbonaceous aerosol in southern Sweden. *Atmos. Chem. Phys.* **2011**, *11*, 11387–11400. [[CrossRef](#)]
56. Yttri, K.E.; Simpson, D.; Nojgaard, J.K.; Kristensen, K.; Genberg, J.; Stenstrom, K.; Swietlicki, E.; Hillamo, R.; Aurela, M.; Bauer, H.; et al. Source apportionment of the summer time carbonaceous aerosol at Nordic rural background sites. *Atmos. Chem. Phys.* **2011**, *11*, 13339–13357. [[CrossRef](#)]
57. Laothawornkitkul, J.; Taylor, J.E.; Paul, N.D.; Hewitt, C.N. Biogenic volatile organic compounds in the Earth system. *New Phytol.* **2009**, *183*, 27–51. [[CrossRef](#)] [[PubMed](#)]
58. Monson, R.K.; Jones, R.T.; Rosenstiel, T.N.; Schnitzler, J.P. Why only some plants emit isoprene. *Plant Cell Environ.* **2013**, *36*, 503–516. [[CrossRef](#)] [[PubMed](#)]
59. Schwarz, J.; Makes, O.; Ondracek, J.; Cusack, M.; Talbot, N.; Vodicka, P.; Kubelova, L.; Zdimal, V. Single Usage of a kitchen degreaser can alter indoor aerosol composition for days. *Environ. Sci. Technol.* **2017**, *51*, 5907–5912. [[CrossRef](#)] [[PubMed](#)]
60. Amato, F.; Viana, M.; Richard, A.; Furger, M.; Prevot, A.S.H.; Nava, S.; Lucarelli, F.; Bukowiecki, N.; Alastuey, A.; Reche, C.; et al. Size and time-resolved roadside enrichment of atmospheric particulate pollutants. *Atmos. Chem. Phys.* **2011**, *11*, 2917–2931. [[CrossRef](#)]
61. Lui, K.H.; Bandowe, B.A.; Ho, S.S.; Chuang, H.C.; Cao, J.J.; Chuang, K.J.; Lee, S.C.; Hu, D.; Ho, K.F. Characterization of chemical components and bioreactivity of fine particulate matter (PM<sub>2.5</sub>) during incense burning. *Environ. Pollut.* **2016**, *213*, 524–532. [[CrossRef](#)] [[PubMed](#)]
62. Lung, S.C.C.; Kao, M.C. Worshipper's exposure to particulate matter in two temples in Taiwan. *J. Air Waste Manag. Assoc.* **2003**, *53*, 130–135. [[CrossRef](#)] [[PubMed](#)]
63. Shi, Y.; Lau, K.; Ng, E. Incorporating wind availability into land use regression modelling of air quality in mountainous high-density urban environment. *Environ. Res.* **2017**, *157*, 17–29. [[CrossRef](#)]
64. Wolf, K.; Cyrus, J.; Hrciniková, T.; Gua, J.; Kusch, T.; Hampel, R.; Schneider, A.; Peters, A. Land use regression modeling of ultrafine particles, ozone, nitrogen oxides and markers of particulate matter pollution in Augsburg, Germany. *Sci. Total Environ.* **2017**, *579*, 1531–1540. [[CrossRef](#)]

